Theoretical Considerations of Membrane Fouling and Its Treatment with Immobilized Enzymes for Protein Ultrafiltration

J. A. HOWELL and O. VELICANGIL,* *Department of Chemical Engineering, University College of Swansea, Swansea SA2 8 PP, United Kingdom*

Synopsis

The ultrafiltration process was modelled in three separate stages with distinctive time constants. It was shown that in the first stage lasting less than 5 s a quasi-steady-state concentration profile is reached on the membrane/solution interface. In the second stage of 1–10-min solute adsorption on the membrane surface including the pores controls the permeation rate. The third stage is governed by a reaction mechanism which produces a surface gel causing flux decline at a slower rate than in the previous adsorption step. This polymerization of the protein to a gel on the membrane was shown to be second order in the interface protein concentrations. A reproducible and inexpensive method has been developed to attach food-grade proteases onto UF membranes by producing a primary adsorbed layer of enzyme which then retards the rate of gel formation on the ultrafilter. This resulted in 25–78% improvement in cumulative permeate yield in a standard 22-h run when processing 0.5% albumin or hemoglobin. The enhanced fluxes with self-cleaning membranes were modelled by incorporating an enzyme activity term to counteract the deposition of gel on the membrane surface and altering the apparent order of the gelation reaction.

INTRODUCTION

Ultrafiltration has gained considerable importance over the past decade partly due to its low energy requirements, athermal character, and simplicity and partly due to the replacement of cellulosic membranes by other polymers of superior properties. On the other hand, the major drawback of this separation process is the significant flux losses encountered during separation and concentration of macromolecular solutions and colloidal suspensions. Although the detergents and dilute acids or bases used for cleaning restore the flux to its original value, a sharp decay occurs within the first few hours of the new run, thus reducing the flux to around 50% of the start-up level.[1,2] This has been attributed to a gel layer formed as a result of concentration polarization of macrosolute molecules rising to a gel concentration at the membrane/solution interface where gel is deposited[3,4] and subsequently consolidated.[2]

The methods reported so far to cure the declining permeation rates can be classified as physical and chemical in nature. Lefebvre et al.[5] observed a sudden recovery of the flux when they reversed the position of their polyamide membrane during ultrafiltration. Lee and Merson[6] suggested a series of chemical treatments of cheese whey prior to ultrafiltration such as lowering the process pH, addition of calcium-sequestering agents or compounds to modify specific protein side chans, or increasing the ionic strength of the feed solution.

* Present address: Institute of Preventive and Social Medicine, Istanbul University, Halk Sağlığı Kürsüsü, Yeni Bina, Capa, Istanbul, Turkey.

Journal of Applied Polymer Science, Vol. 27, 21–32 (1982)

CCC 0021-8995/82/010021-12$01.20

Fisher and Lowell[7] suggested the use of immobilized proteases to enhance the permeation rates of a reverse osmosis membrane for sewage treatment. They attached trypsin into a membrane cast from modified cellulose acetate, but did not report any flux test with sewage. The preparation of self-cleaning UF membranes by attaching papain on their surfaces was reported by Velicangil and Howell.[1] When tested with cheese whey, these membranes exhibited higher cumulative permeate yields during 28-h or 78-h runs with respect to their controls.

The purpose of this study was to develop a comprehensive model for the ultrafiltration process which would elucidate the different stages of the complex flux drop phenomenon as well as to progress in the design and applications of self-cleaning UF membranes. A true understanding of the gel layer formation phenomenon would consequently provide the means to circumvent the flux decay, regarded as the nuisance of this novel separation process.

EXPERIMENTAL

Materials

Amicon Diaflo membranes were used throughout this work (supplied by Amicon Ltd., High Wycombe, England). The two letters in the membrane code signify the material of the membrane and the two figures indicate its nominal molecular cutoff in terms of kdaltons. Of the PM series, made of polysulfone, PM-10 and PM-30 membranes were employed.

Bovine Albumin (Cohn Fraction V) and hemoglobin (crude type) were purchased from Sigma London Chemical Co., Poole, Dorset. Corolase S100 (industrial papain produced from carica papaya, purified and activated by purosulfite) and Proteinase P (a neutral protease complex, from *Aspergillus* cultures) were generously donated by Röhm GmbH, Darmstadt, West Germany. All crude enzymes were food grade.

Equipment

The ultrafiltration cell was a flat thin-channel spiral type with 1.5-cm channel depth and 150 mm in diameter. It was connected to a centrifugal pump which delivered the feed solution up to 400 kPa at 5 L/min. The system was operated at total recycle with permeate and retentate returned and thoroughly mixed in the feed reservoir. Temperatures and pH were controlled, the probes being installed in the feed tank.

Ultrafiltration experiments were conducted at 25°C or 30°C and at $R_e = 6000$. The average transmembrane pressure was maintained between 207 kPa and 221 kPa.

Methods

The following procedure was employed to introduce proteases onto ultrafiltration membranes: The enzyme was dissolved in acetate buffer (pH 4.0) to a concentration close to the concentration of the protein source to be separated, which usually varied between 0.2% and 0.5%. This solution was ultrafiltered

through the membrane at total recycle in the main unit until the permeate flux reached a steady value over the short term (usually 6–12 min). The ultrafiltration conditions were the same as for the succeeding main separation stage. Then, for 4–5 min, water was recirculated to purge the free enzyme from the system.

For some experiments a 0.125% glutaraldehyde solution in phosphate buffer (pH 6.5) was subsequently circulated for 45 min to crosslink and hence chemically immobilize the enzyme. The excess glutaraldehyde was then reduced by perfusion with 0.05 M $NaBH_3$. The recirculation rate of $NaBH_4$ was kept low (200 mL/min) in comparison with those of enzyme and glutaraldehyde solutions (2600 mL/min) due to the difficulty in pumping the evolved hydrogen through the system. At the end of a daily 20–22-h UF run, the exhausted enzyme was removed from the membrane together with protein deposits by detergent cleaning using 0.3% "Tergazyme" (Alconox Inc., New York, N.Y.).

For certain prototype runs with papain-adsorbed membranes the feed solution contained 0.005 M cystein and 0.002 M EDTA as activators.

Automated amino acid analyses were carried out on the permeate and also on the retentate to determine the extent of hydrolysis of the processed protein by the membrane-bound enzymes.

RESULTS AND DISCUSSION

Mathematical Model

Ordinary Membranes

For a parallel plate system, the buildup of wall concentration C_w which is the solute concentration at the upstream surface and its approach to the limiting gel concentration C_g were analyzed by using a dynamic model. The continuity equation for solute in this system for the unsteady state, ignoring convection in the longitudinal direction and assuming constant transverse velocity, can be written as

$$\frac{\partial C}{\partial t} = D\frac{\partial^2 C}{\partial y^2} - v\frac{\partial C}{\partial y} \tag{1a}$$

with the initial and boundary conditions

$$t = 0, \quad C = C_b \tag{1b}$$

$$y = 0, \quad C = C_b \tag{1c}$$

$$y = L, \quad D\frac{\partial C}{\partial y} = vC \tag{1d}$$

where C is the local solute concentration, L is the boundary layer thickness, D is the solute diffusion coefficient, y is the distance into the boundary layer, and C_b is the bulk solution concentration. C_w is the solute concentration at the wall ($y = L$) which is given by

$$\frac{C_w}{C_b} = \exp\left(\frac{vL}{D}\right) + \sum_{n=1}^{\infty} A_n \exp\left(-\lambda_n^2 t\right) Y_n\left(\frac{\lambda_n^2 D}{v^2}, \frac{vL}{D}\right) \tag{2}$$

where the A_n are constants and λ_n and Y_n are the eigenvalues and eigenfunctions, respectively, of the Sturm–Liouville problem associated with eq. (1).

This analytical solution was matched with ultrafiltration data for papain. For D (25°C) = 10.3×10^{-11} m^2/s and $v = 5.8 \times 10^{-5}$ m^2/s (initial experimental transmembrane velocity), $\lambda_1^2 = 2.54$/s and $\lambda_2^2 = 8.06$/s, and it was shown that over 99.9% of the gelling concentration was reached in 2.72 s, irrespective of the assumed gelling concentration C_g, provided that the chosen initial value of v is consistent with the one computed from the steady-state solution of eq. (1). As at $y = L$ $\Sigma A_n \cdot Y_n = -C_b \cdot \exp(vL/D) + (-C_g)$ and neglecting terms higher than the first, eq. (2) takes the form

$$C_w = C_b \exp\left(\frac{vL}{D}\right) - C_b \exp\left(\frac{vL}{D}\right) \exp(-\lambda_1^2 t) \tag{3}$$

The time needed for 99.9% of the gelling concentration to be reached at the wall is then computed from

$$\exp(-\lambda_1^2 t) = 0.001 \quad \text{with } \lambda_1^2 = 2.54/\text{s}.$$

The mass transfer coefficient for solute transport away from the membrane surface was calculated from the Dittus–Boelter correlation for turbulent flow in thin channels

$$k_m = 0.02 \frac{Q^{0.8} D^{0.67}}{b w^{0.8} \nu^{0.47}} \tag{4}$$

where Q is the volumetric flow rate (43.3×10^{-6} m^3/s), b is the channel depth (1.5×10^{-3} m), w is the channel width (12×10^{-3} m), ν is the kinematic viscosity (1×10^{-6} m^2/s).

Setting $k_m = D/L$, the boundary layer thickness was evaluated. For the system investigated, $k_m = 1.26 \times 10^{-5}$ m/s and L = 5.12×10^{-6} m. Since the calculated time taken to reach 99.9% of the steady state concentration is so short compared to the time constants observed experimentally for flux decay, it seems that the assumption of constant flux [v in eq. (1)] is justifiable.

The sharp flux drop observed within the next 10 min is attributed to the adsorption of solute onto the membrane in the regions of the pores. Although the adsorption phenomena on ultrafilters has been emphasized by many researchers,[8–10] the available data is inadequate to establish the kinetics of this process. The flux over the initial 11 min of ultrafiltration of a 0.2% papain solution through a PM-30 membrane is presented in Figure 1. The change in solute concentration in the permeate during this initial period is also plotted. The effect of primary adsorption of the solute in the membrane pores was very pronounced as the equivalent diameter of the papain molecule (4.0 nm), and the apparent diameter of a PM-30 membrane (4.7 m) are very close. After rising for the first minute the papain concentration in the permeate then fell off slightly and remained stable for the rest of the 20-h run (not shown in the graph).

Table I summarizes some of the adsorption experiments on ultrafiltration membranes and hollow fibres. A water flux drop between 35% and 49% was observed presumably due to the adsorption at atmospheric pressure prior to the run or to the adsorption under pressure during the run. An important feature of the last three experiments performed under pressure was that because of concentration polarization the actual adsorbate concentration to which the membranes were exposed was much higher than the reported bulk concentration. Ingham and his co-workers[10] reported that adsorbate protein bulk concentrations

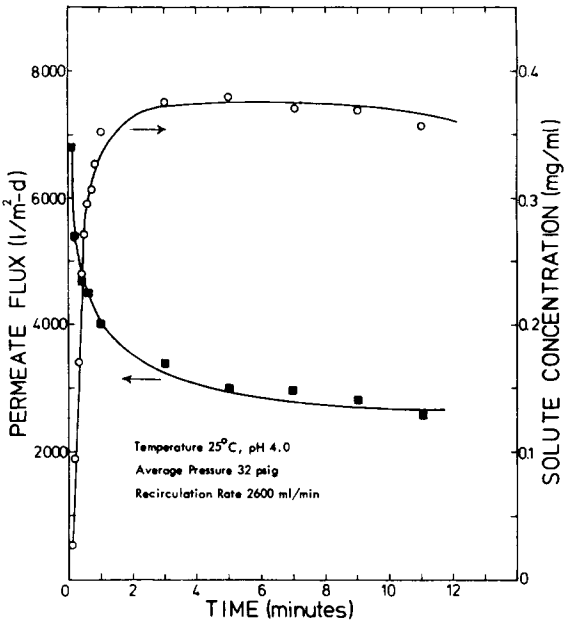

Fig. 1. Initial rate and solute concentration of the papain permeate: PM-30 membrane.

between 0.001 mg/mL and 0.01 mg/mL produced sufficient adsorption to reduce the permeate flux by 37%. This leads to the obvious conclusion that in ultrafiltration almost all the practical range of bulk concentrations is sufficient to cause adsorption on the membrane and conseqently reduce the flux up to 49%.

It is suggested that the third stage of the process is dominated by the polymerization mechanism. This third stage is characterized by deposition of the gel on the membrane surface at a much slower rate than in the previous adsorption stage. It produces an increasing thickness of gel layer due to chemisorption and continues for several hours. This work assumed that it occurred as an nth order reaction with respect to C_w and the best value of the index n was obtained from data fitting.

The gel layer thicknesses corresponding to decreasing permeate fluxes with time were evaluated from

$$v = \frac{\Delta P}{\mu(R_m + l/P_g)} \tag{5}$$

where ΔP is the transmembrane pressure drop, μ is the bulk viscosity, l is the gel layer thickness, and P_g is the permeability of the gel of concentration C_g. The term l/P_g is the gel layer resistance R_g and acts in series with the membrane resistance R_m to reduce the solvent flux through the membrane.

The Kozeny equation[11] for porous solids was used as an approximation for estimating the gel permeability:

$$P_g = \frac{d^2}{180} \frac{\epsilon^{-3}}{(1 - \bar{\epsilon})^2} \tag{6}$$

assuming spherical shape for the particles in the layer. Particle diameter is

TABLE I
Protein Adsorption on Membranes

No.	Membrane	Adsorbate protein	Yield ($\mu g/cm^2$)	Adsorption parameters					Solvent flux drop due to adsorption (%)
				Pressure (kPa)	Temperature (°C)	pH	Time (min)	Adsorbate conc (mg/mL)	
1	PM-10[a]	Papain	4.8	0	4	4.0	60	1.0	40[b]
2[c]	PM-10[a]	Papain	68	0	4	6.2	120	1.0	49[b]
3[c]	PM-10[a]	Papain	88	0	4	6.2	120	1.0	35[b]
4[d]	XP-50	BSA	175	80	25(?)	5.0	65	5.0	—
5[d]	PM-30	BSA	—	137(?)	—	—	—	0.005	37
6	PM-30	Papain	—	206	25	4.0	6	2.0	43[e]
7	XM-100	Whey protein	—	0	50	6.2	3	6.0	22[f]

[a] Pretreated in 3*N* HCl, 50°C for 45 min to 1 h.
[b] Cheese whey flux relative to the control.
[c] Velicangil and Howell.[1]
[d] Ingham et al.[10]
[e] Adsorbate solution flux.
[f] Water flux.

denoted by d and $\bar{\epsilon}$ is the porosity of the gel. The gel layer thicknesses computed via eq. (5) usually had the same order of magnitude as that of the membrane skin thicknesses ($\sim$1 μm).

A computer program to process data by nonlinear optimization with the least squares technique was used to find the polynomial giving the best fit to the experimental results. This was found to be a second order curve of parabolic shape:

$$t = a_0 + a_1 + a_2{}^2 \tag{7}$$

The time derivatives d/dt from this equation were calculated at certain intervals and plotted against C_w, evaluated from

$$C_w = C_b \exp(v/km) \tag{8}$$

for the corresponding transverse velocities. Equation (8) is the steady-state solution of eq. (1a) with the boundary conditions

$$y = 0, \quad C = C_b \tag{9a}$$

$$y = L, \quad C = C_w \tag{9b}$$

and k_m was calculated from the Dittus–Boelter correlation for turbulent flow in thin channels [eq. (4)]. The flux loss due to the polymerization of deposit with time was envisaged as an infinite series of successive steady states, each of which had a smaller wall concentration than the previous one as implied by eq. (8). The log–log plots of C_w vs. the rate of gel layer formation dl/dt for cheese whey and 0.5% albumin solution were obtained using the same nonlinear optimization technique on the computer and are presented in Figures 2(a) and 2(b), respectively. The analysis of these two sets of data yielded a second order relationship between the gel layer growth rate and the wall concentration C_w:

$$\frac{dl}{dt} = k_r C_w{}^2 \tag{10}$$

Combining eq. (5) and 980 with eq. (10) yields

$$\frac{dl}{dt} = k_r C_b^2 \exp\left[2\Delta P/k_m \mu \left(R_m + \frac{l}{P_g}\right)\right] \tag{11}$$

The order n of the polymerization reaction evaluated from the best fit in Figures 2(a) and (b) is 1.946 for cheese whey and 2.035 for bovine albumin ultrafiltration. The calculated values for k_m using the Dittus–Boelter correlation [eq. 4)] are 1.52×10^{-5} m/s for cheese whey at 50°C and 1.725×10^{-5} m/s for albumin at 25°C. In both cases the recirculation rate was 2600 mL/min. The diffusivity value used for cheese whey proteins at 50°C was 3.75×10^{-11} m^2/s. This figure is quite low when compared with the diffusivity 11.7×10^{-11} m^2/s of albumin (MW 68,000) at 50°C and also lower than the weighted average of the diffusivities of cheese whey proteins, but the electromicrographs presented by Lee and his co-workers[6,12,13] are excellent evidence for the high polymer nature of cheese whey proteins depositing on the membrane surface. The generally lower permeation rate of cheese whey ultrafiltration in comparison with other single protein sources under the same conditions is also indicative of a lower mass transfer coefficient for back diffusion. Hence it appears that gel layer formation of cheese whey is governed either by a second order mechanism (assuming the

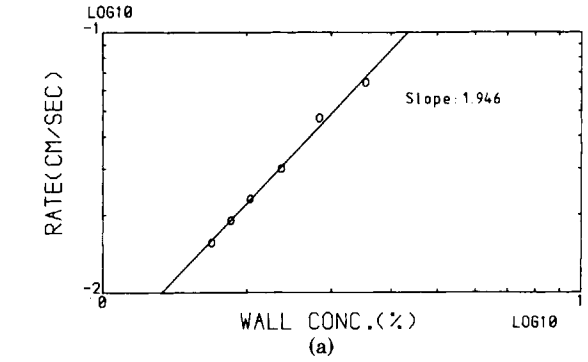

(a)

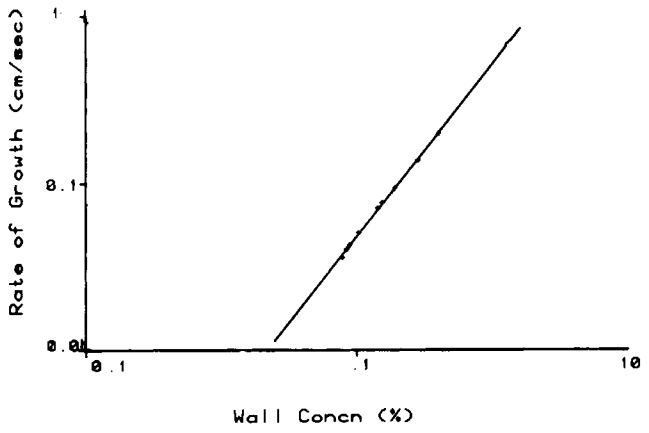

(b)

Fig. 2. Variation of gel layer thickness with time: (a) cheddar cheese whey; (b) 0.5% albumin solution.

above diffusivity value is a valid one) or by a higher order. However, a variation in the diffusivity induces a change in the slope of the curve in Figure 2(a) and thus the value of n without affecting the correlation.

Self-Cleaning Membranes: Theory

The enhanced fluxes were modelled by modifying the original eq. (10) for gel deposition. An experimental run carried out over 55 h with a PM-10 membrane activated with a fungal proteinase filtering albumin showed that the rate of gel deposition was given by

$$\frac{d}{dt} = k_r C_w - k_e \tag{12}$$

where k_e is the rate of protein removal by the attached enzyme.

By substituting eq. (5) into eq. (12), we obtain the following expression for the rate of gel layer growth:

$$\frac{dl}{dt} = k_r C_b \exp\left|\Delta P / k_m \mu \left(R_m + \frac{l}{P_g}\right)\right| - k_e \tag{13}$$

Using the same computer program as before for nonlinear optimization by least squares, the parameters k_r and k_e of eq. (13) were evaluated. It is hard to see why the apparent order of reaction should change with the activated membrane although the second rhs term in eq. (1) could represent decomposition of builtup gel by the enzyme. A correlation of 0.99992 was found when fitting using eq. (1) to relate C_w data to smoothed data for dl/dt. The run with papain-pretreated membrane (I1) requires a more complex model as activators (cysteine and EDTA) were involved in the system.

The acceptability of the gel polarization theory has been substantiated by the success with which it has been applied to the analysis of flux vs. concentration data. But it ignores the effects of polarization on the sieving properties of the membrane and also its predictions about the unsteady-state flux behavior are speculative as they do not stem from the transient solution of the solute conservation equation at the membrane surface [eq. (1)]. Gel polarization theory differs from the present model in that it ascribes the rapid flux drop over the first minute as being due to convective gel deposition from a wall concentration C_g while the concentration profile is still in the unsteady state. In this initial period all the gel is assumed to form, and the later slower flux decay is ascribed to the hardening of the gel.

Self-Cleaning Membranes: Experimental

The attachment of proteases onto membranes prior to the ultrafiltration can be considered analogous to the rapid initial adsorption of protein during ultrafiltration. In this respect, the results presented in this section also support the validity of the adsorption phenomenon besides providing a convenient method to combat the declining permeation rates when processing macromolecules.

A primary adsorption layer of enzyme was produced instead of one of processed protein during the first minutes of the run. This was accomplished by ultrafiltering a protease solution for 6–12 min prior to each run. The enzyme precoat partially hydrolyzed the solute molecules deposited later thus retarding the rate of formation of gel layer on the membrane and around the pores.

In these experiments either the same membrane was used in an alternating way as prototype (enzyme attached) and then as control or two different membranes with identical histories were employed as prototype and as control respectively.

The flux behavior of self-cleaning membranes is illustrated in Figures 3 and 4. The activated prototype in Figure 3 showed 44% improvement in total permeate over the control. The flux loss of the prototype over the 22-h run was only 18% against the 55% flux decline of the control during the same period. In another run of the prototype without activators a 31% increase in permeate yield was obtained, although after the first 6 h the flux decline accelerated, presumably due to the rapid inactivation of papain, and the final flux value matched the 22-h value of the control. The fourth experiment was designed to distinguish whether the flux enhancements with various prototypes were due to the physical effect of the adsorbed papain layer as a prefilter coat or due to its biochemical action. To this purpose, 0.002 M H_2O_2 instead of the activators was introduced into the feed solution to inactive papain completely. After 6 h the feed solution was replaced by a fresh batch containing activators and no H_2O_2. Although up to this

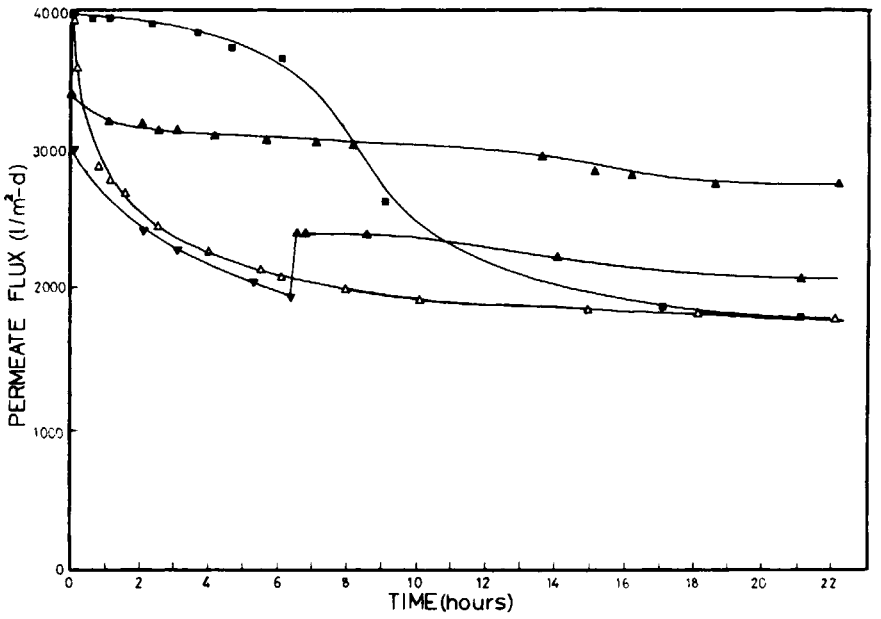

Fig. 3. Effect on flux of activation with cysteine, with and without previous inactivation with H_2O_2: PM-30 membrane, BSA. (△) Control, D1; (■) prototype (not activated), C2; (▲) prototype (activated), E1; (▼/▲) prototype (inactivated/activated), F1.

point the rate of flux decline was identical with the control, a sudden recovery was observed and the cumulative permeate was 13% higher within the next 16 hr. A similar experiment, but reversing addition of H_2O_2/activators order, was performed with 0.5% hemoglobin ultrafiltration (Fig. 4). After 3 h of operation

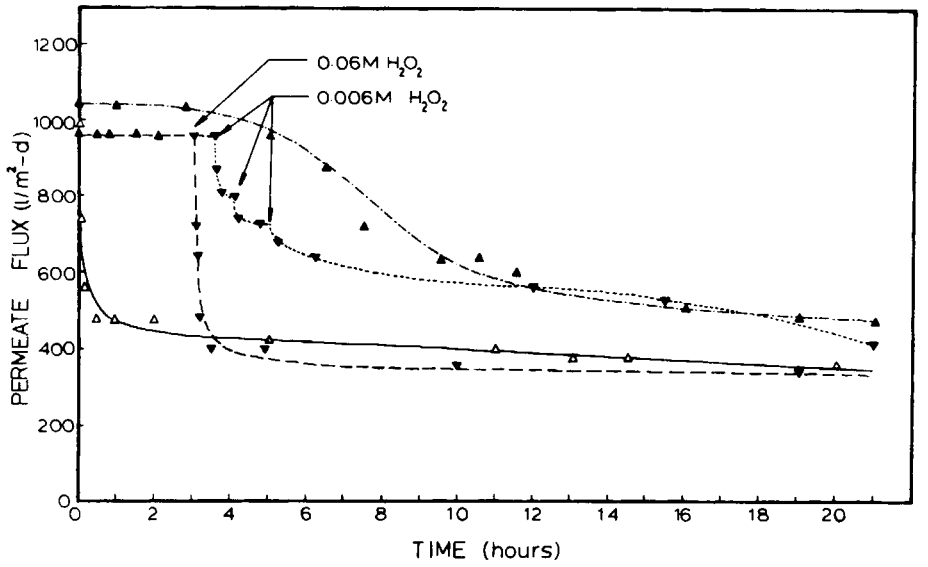

Fig. 4. Effect on flux of H_2O_2 inactivation during run: PM-10 membrane, hemoglobin. (△) Control, G2; (▲) prototype (activated), G1; (▲/▼) prototype (activated/inactivated), G3; (▲/▼) prototype (activated/inactivated), G4.

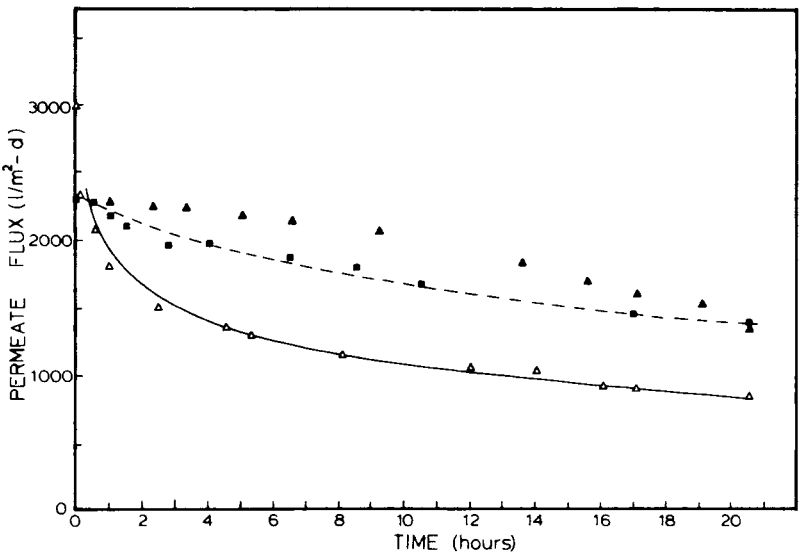

Fig. 5. Modelling flux of prototype and control/effect of different enzymes: PM-10 membrane, BSA. (△) Control, H1; (▲) papain (Corolase S100), I1; (■) fungal proteinase P, H2; (---) model.

with activators, where the flux was constant and had identical behavior with that of papain-adsorbed and -activated membrane, 0.06 M H_2O_2 was introduced into the system. A sudden drop in the flux was observed, and it showed similar behavior to that of the control for the rest of the run. When three portions of 0.006 M H_2O_2 was added at hourly interrvals, there were corresponding flux decreases. Also, the most striking flux difference between the prototype and the control (same membrane) was achieved with a hemoglobin solution. Over a 21 h run the cumulative permeate showed 78% improvement.

Fungal proteinase P was attached onto a PM-10 membrane and used for ultrafiltration of 0.5% bovine albumin (Fig. 5). A 50% improvement in total permeate yield was obtained over 20.5 h. This compare well with that of papain adsorbed and activated membrane (71% improvement) considering that this neutral protease does not require activation. The difference in improvement between the two types of membranes is also in accord with the free solution activities of the corresponding enzymes.

The net protein loss through the membrane due to cleavage of filtered albumin by the active enzyme was found to be around 4% of the total during the 10 times concentration of a batch at the permeation rates illustrated in Figure 5.

This research was sponsored by the Science Research Council of United Kingdom under Grants No. G/RA/2555.7 and G/RA/88897.

References

1. O. Velicangil and J. A. Howell, *Biotechnol. Bioengr.*, **19**, 1891 (1977).

2. W. F. Blatt, A. Dravid, A. S. Michaels, and L. Nelson, in *Membrane Science and Technology*, J. E. Flinn, Ed., Plenum, New York, 1970, pp. 47–97.

3. A. S. Michaels, *Chem. Engr. Progr.*, **64**(12), 31 (1968).

4. M. C. Porter and L. Nelson, in *Recent Developments in Separation Science*, Vol. 2, N. N. Li, Ed., Chem. Rubber Publ. Co., Cleveland, Ohio, 1973, pp. 227–267

5. M. S. Lefebvre, C. J. D. Fell, A. G. Fane, and A. G. Waters, in *Ultrafiltration Membranes and*

Applications, A. R. Cooper, Ed., Polymer Science and Technology, Vol. 13, Plenum, New York, 1980, pp. 79–98.

6. D. N. Lee and R. L. Merson, *J. Food Sci.*, **41,** 778 (1976).
7. B. S. Fisher and J. R. Lowell, Jr., "New Technology for Treatment of Wastewater by Reverse Osmosis," Report to EPA on FWQA Program, 1970.
8. J. D. Ferry, *Chem. Rev.*, **18,** 373 (1936).
9. C. W. Hancher and A. D. Ryan, *Biotechnol. Bioengr.*, **15,** 677 (1973).
10. K. C. Ingham, T. F. Busby, Y. Sahlestrom, and F. Castino, in *Ultrafiltration Membranes and Applications*, A. R. Cooper, Ed., Polymer Science and Technology, Vol. 13, Plenum, New York, 1980, pp. 141–158.
11. J. Happel and H. Brenner, *Low Reynolds Number Hydrodynamics*, 2nd ed., Noordhoff Int. Publ., Leyden, 1965.
12. D. N. Lee, M. G. Miranda, and L. M. Merson, *J. Food Technol.*, **10,** 139 (1975).
13. D. N. Lee and R. L. Merson, *J. Food Sci.*, **41,** 603 (1976).

Received July 18, 1980
Accepted April 27, 1981